Mechanical Properties of Blends of Nylon 6 with a Chemically Modified Polyolefin

HSIAO-KEN CHUANG and CHANG DAE HAN, *Department of Chemical Engineering, Polytechnic Institute of New York, Brooklyn, New York 11201*

Synopsis

Both tensile and impact properties were measured of a heterogeneous polymer blend system, consisting of nylon 6 and a chemically modified polyolefin, DuPont CXA3095, which is an ethylene-based multifunctional polymer. It was found, from the tensile testing, that the blends exhibited no signs of necking, and the addition of a soft resin (CXA3095) reduced the modulus and the tensile strength of nylon 6, whereas the percent elongation at break went through a minimum. When 20 wt % of CXA3095 was added to nylon 6, the impact strength was increased approximately three times. When the factors describing the interfacial adhesion were incorporated, the existing models for predicting the tensile modulus of blends were found to describe the experimental data rather well. In order to help explain the mechanical behavior observed, photomicrographs were taken of the fracture surfaces, using a scanning electron microscope.

INTRODUCTION

In the past, some attempts have been made to correlate the morphology of heterogeneous polymer blends with their mechanical/physical properties in the solid state. Merz and co-workers[1] have reported physical/mechanical properties together with the morphology of blends of polystyrene with butadiene. They reported that the impact resistance of the dispersed phase is higher than that of the continuous phase, and showed that the tensile energy absorbed by the dispersed particles is higher than that absorbed by the continuous phase, on an equal volume basis. They were successful in showing the qualitative relationship between the blend's microstructure and its mechanical properties. Rovatti and Bobalek[2] have also reported the physical/mechanical properties of a polymer blend of poly(vinyl chloride)/nitrilebutadiene rubber, together with photomicrographs of molded specimens. They showed how the physical/mechanical properties of their systems were improved as the state of mixing was improved or as the processing temperature was increased. Giuffria[3] has also reported mechanical property-morphology relationships in high-impact polystyrene. He described methods for obtaining high gloss impact-modified polystyrene by changing the processing technique, and thus influencing the microstructure of the final products.

Also, some efforts have been spent on developing theories[4-10] for predicting the mechanical (static or dynamic) properties of polymer–particulate or polymer–polymer composites, and experimental studies[11-16] have been carried out to test the theories. At present, however, there is no comprehensive theory which predicts the mechanical/physical properties of a heterogeneous polymer blend in terms of its processing variables.

Journal of Applied Polymer Science, Vol. 30, 165–177 (1985)
 CCC 0021-8995/85/010165-13$04.00

In recent years, coextruded films consisting of nylon 6 and a modified polyethylene have been widely used in the packaging industry. The scraps generated from this process pose a formidable task for disposal. A possible use of the scraps may be found in reprocessing them for producing blends, which hopefully possess acceptable mechanical properties.

Having conducted coextrusion research with nylon 6 and a chemically modified polyolefin (i.e., DuPont, CXA3095),[17] we were motivated to investigate the mechanical properties of the blends prepared from these two polymers. Our approach was parallel to the concept of rubber toughened nylon. That is to say, when a rubbery component is dispersed in a rigid nylon matrix, the rubber phase acts as an effective stress concentrator and enhances both crazing resistance and shear yielding by absorbing a large amount of impact energy.

THEORETICAL BACKGROUND

Many theories have been advanced for predicting the elastic modulus of two-phase blends. According to Dickie,[18] these theories can be divided into three groups: (1) mechanical coupling model; (2) self-consistent model; and (3) bounds on the modulus. The mechanical coupling model is an empirical expression, containing an adjustable parameter. The major drawback to using this model is attaching a physical meaning to the adjustable parameter. The self-consistent model is based on the following assumptions: (1) Perfect adhesion exists between the matrix and the inclusion; (2) interinclusion interactions are negligible; (3) the inclusions embedded in a matrix are spherical in shape and are isotropic morphologically and mechanically.

The Kerner model[7] was originally developed for the shear modulus of a composite consisting of particulates and polymer matrix, but the model may be useful to predict the tensile modulus of a certain class of heterogeneous blend systems. When the matrix and inclusion have the same Poisson's ratio, the Kerner model may be written as[7]

$$E_b = E_m \left\{ \frac{\phi_d E_d/[(7 - 5\nu_m)E_m + (8 - 10\nu_m)E_d] + \phi_m/15(1 - \nu_m)}{\phi_d E_m/[(7 - 5\nu_m)E_m + (8 - 10\nu_m)E_d] + \phi_m/15(1 - \nu_m)} \right\} \quad (1)$$

for a system having perfect adhesion at the boundary. Note that the Poisson's ratios of nylon 6 and CXA3095, respectively, are 0.44 and 0.5. These values are close enough for us to use the Kerner equation in this form. Here E is the tensile modulus, ϕ is the volume fraction of the discrete phase, and ν is Poisson's ratio. The subscripts b, m, and d refer to the blend, the matrix, and the dispersed phase, respectively. For foams, rubber-filled rigid polymers, or systems in which the inclusions are loosely bound, $E_d \cong 0$ and eq. (1) reduces to

$$\frac{1}{E_b} = \frac{1}{E_m}\left[1 + \frac{15(1 - \nu_m)}{(7 - 5\nu_m)}\frac{\phi_d}{\phi_m}\right] \quad (2)$$

Note that, in Kerner's derivation, only particle–matrix adhesion, but no particle–particle interaction, was assumed. Therefore, from the point of view of rigor, the Kerner model may not be applicable to the polymer blend

systems in which strong interactions between the inclusions and the matrix may exist. For such situations, Nielsen[19] suggested a modification of the Kerner model.

According to Nielsen,[19] we have the following expressions.

(i) For a rigid polymer dispersed in a rubber matrix:

$$\frac{E_b}{E_m} = \frac{1 + AB\phi_d}{1 - B\psi\phi_d} \tag{3}$$

in which

$$B = \left(\frac{E_d}{E_m} - 1\right)\Big/\left(\frac{E_d}{E_m} + A\right), \quad \psi = 1 + \left(\frac{1 - \phi_{\max}}{\phi_{\max}^2}\right)\phi_d$$

(ii) For rubber inclusions in a rigid matrix:

$$\frac{E_m}{E_b} = \frac{1 + AB_i\phi_d}{1 - B_i\psi\phi_d} \tag{4}$$

in which

$$B_i = \left(\frac{E_m}{E_d} - 1\right)\Big/\left(\frac{E_m}{E_d} + A\right), \quad \psi = 1 + \left(\frac{1 - \phi_{\max}}{\phi_{\max}^2}\right)\phi_d$$

$\phi_{\max}$ being the maximum packing volume which can be considered as a scale of the interaction between the two phases. A small value of $\phi_{\max}$ represents a large extent of adherent interphase, which is immobilized by the inclusions. The constant A in eqs. (3) and (4) takes into account the geometry of the particulate phase. For spherical inclusions and for the two phases having the same Poisson's ratio, the constant A equals $(7 - 5\nu_m)/(8 - 10\nu_m)$ for eq. (3) and $(8 - 10\nu_m)/(7 - 5\nu_m)$ for eq. (4).

Paul[20] used the calculus of variations to bound the strain energy and set the limits on the modulus of composites. According to him, the upper bound is given by

$$E_b = (1 - \phi_d)E_m + \phi_d E_d \tag{5}$$

and the lower bound by

$$E_b = 1\Big/\left(\frac{1 - \phi_d}{E_m} + \frac{\phi_d}{E_d}\right) \tag{6}$$

EXPERIMENTAL

Materials. Nylon 6 (American Enka Co.) and CXA3095, a modified polyethylene resin from DuPont, are the resins employed in this study. Four blends, namely, nylon/CXA = 80/20, 60/40, 40/60, and 20/80 by weight,

were prepared in a twin-screw compounding machine (Werner and Pfleiderer ZDSK-53). The compounded pellets were injection-molded to obtain test specimens for measurements of tensile properties and Izod impact test. Before their use, the test specimens were vacuum dried at 70°C for 30 h to remove moisture and to relieve the frozen-in stress. The dried test specimens were stored in a dessicator until their use.

Tensile Properties Measurement. Tensile property experiments were done on an Instron machine at room temperature following the procedure described in ASTM D638. A crosshead speed of 0.508 cm/min was used in all measurements.

Izod Impact Strength Measurement. All the specimens had the dimension 6.35 × 1.27 × 0.635 cm, with a notch 0.0254 cm in radius. Notched Izod impact strength of the blends was measured, using a Baldwin impact testing machine either at room temperature, or, when the samples could not be broken at room temperature, at about −40°C with the aid of dry ice.

Morphological Investigation. The mechanical properties of heterogeneous polymer blends are dependent upon their microstructure, especially the size and shape of the dispersed phase. In order to determine the particle size of the dispersed phase in the specimens and its distribution, photomicrographs were taken with the aid of a phase contrast optical microscope. The specimens were first embedded in an epoxy resin and then microtomed into thin slices of about 3 μm, which were later examined under a microscope.

The fracture topographs as well as the dispersed structure of the fractured specimens were studied, using a scanning electron microscope (SEM) (AMR 1200) operated at 15–25 kV. The surface of the tensile- and impact-fractured specimens were coated with gold to avoid charging under an electron beam.

RESULTS AND DISCUSSION

Tensile Properties

The stress–strain curves for the blend system are shown in Figure 1. It is seen that nylon 6 shows yield behavior. The blends exhibited no signs of necking, and the addition of a soft resin (CXA3095) reduced the modulus and the tensile strength of nylon 6, as summarized in Table I.

When plotted against the weight percent of nylon 6 in the blend, the tensile modulus and tensile strength increase monotonically with the amount of nylon 6, as shown in Figures 2 and 3, whereas the percent elongation at break goes through a minimum as shown in Figure 4.

The theoretical predictions of the modulus [see eqs. (1)–(6)] on the basis of the various theories discussed above, are given in Figure 2, together with the experimental data. Since the mechanical properties of heterogeneous polymer blends are dependent upon the microstructure, the morphological structure should be examined before the modulus behavior is discussed.

The morphological investigation revealed that the domain structure strongly depends on the amount of the dispersed phase present in the blend. The domains are mostly spherical in shape as shown in Figure 5, obtained

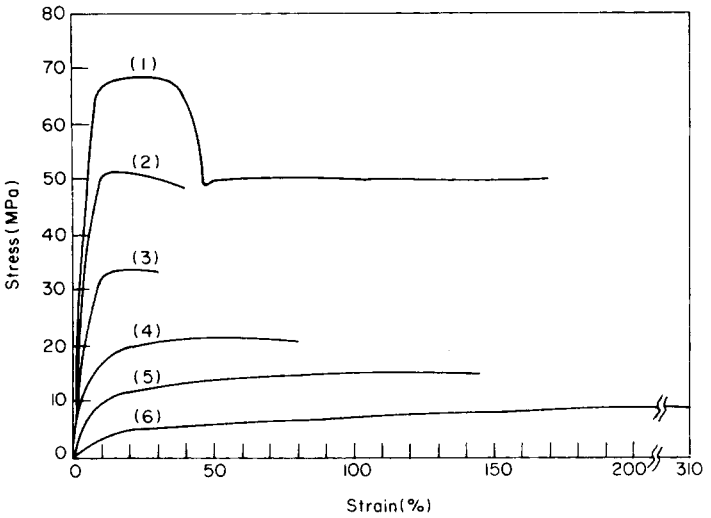

Fig. 1. Stress–strain curves for blend system with a crosshead speed of 0.508 cm/min: (1) nylon 6; (2) nylon 6/CXA 3095 = 80/20; (3) nylon 6/CXA 3095 = 60/40; (4) nylon 6/CXA 3095 = 40/60; (5) nylon 6/CXA 3095 = 20/80; (6) CXA 3095.

by phase contrast optical microscopy, and in Figure 6 obtained by SEM on the cryogenically fractured surface. From the micrographs, the following features may be observed: (1) For the CXA-rich blends, the nylon 6 forms the discrete phase (dark area) and is dispersed in the CXA matrix, and, for the nylon-rich blend, the CXA3095 forms the discrete phase (white area) and is dispersed in the nylon phase; (2) the size distributions of the discrete phase are fairly narrow, and the domain (or particle) size of the discrete phase varies, to a large extent, with the blend composition. The particle size in the nylon/CXA = 20/80 blend is much smaller than that in the nylon/CXA = 80/20 blend. This is believed due to the melt viscosity of the nylon 6 employed, which is lower than that of CXA3095. (3) In either the nylon-rich or CXA-rich blends the discrete phase is tightly bound to the continuous phase.

TABLE I
Tensile Properties of Blend System at a Crosshead Speed of 0.508 cm/min

Blends composition (by wt)	Tensile strength (MPa)	Elongation at break (%)	Tensile modulus (MPa)	Volume fraction of nylon[a]
Nylon 6	68.5	170	1020	1.000
Nylon/CXA = 80/20	51.5	40	786	0.767
Nylon/CXA = 60/40	33.5	30	473	0.553
Nylon/CXA = 40/60	21.5	80	260	0.354
Nylon/CXA = 20/80	15.2	145	93	0.170
CXA3095	9.4	310	37	0.000

[a] Density of nylon 6 = 1.15 g/cm^3, density of CXA 3095 = 0.95 g/cm^3.

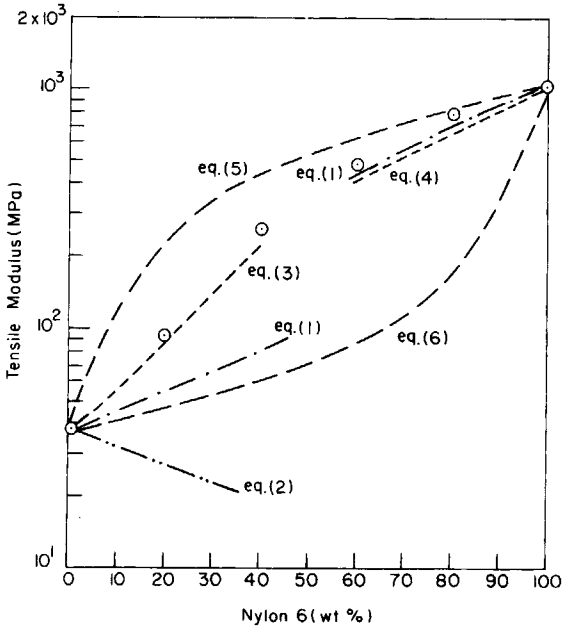

Fig. 2. Tensile modulus versus blend composition for the nylon/CXA blends: (⊙) experimental data; (— — —) Paul's upper and lower bounds; (– · – · –) Kerner's model with perfect adhesion; (– ·· – ·· –) Kerner's model with foam or loosely bound inclusions; (- - - - -) Nielsen's model.

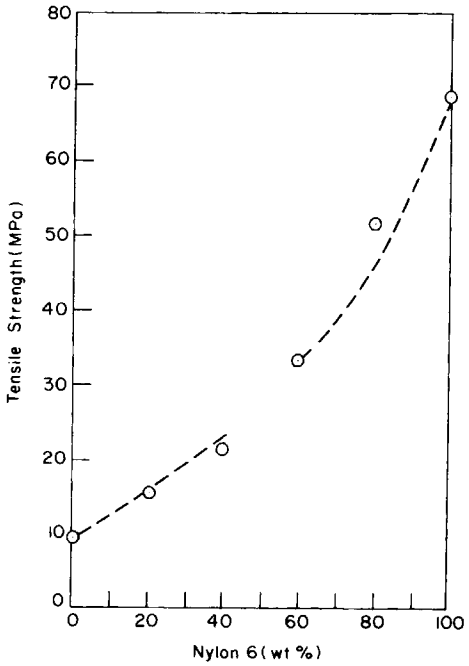

Fig. 3. Tensile strength versus blend composition for the nylon/CXA blends: (○) experimental data; (- - -) theoretical prediction based on the tensile strength proposed by Nielson.

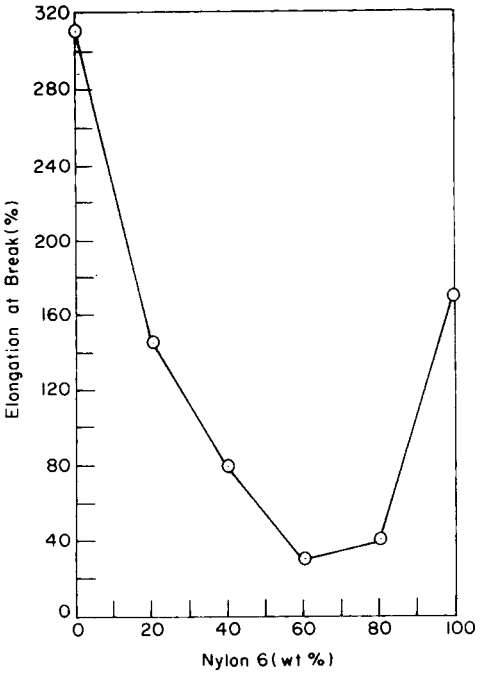

Fig. 4. Percent elongation at break versus blend composition for the nylon/CXA blends.

Referring to Figure 2, since the tensile modulus of CXA3095 is very low compared to that of the nylon 6, CXA3095 contributes little to the overall modulus when it is dispersed in the nylon matrix. Thus, for the nylon-rich blend, the Kerner model, eq. (1), and the Nielsen model, eq. (4), predict the experimental data rather well. On the other hand, when CXA3095 forms

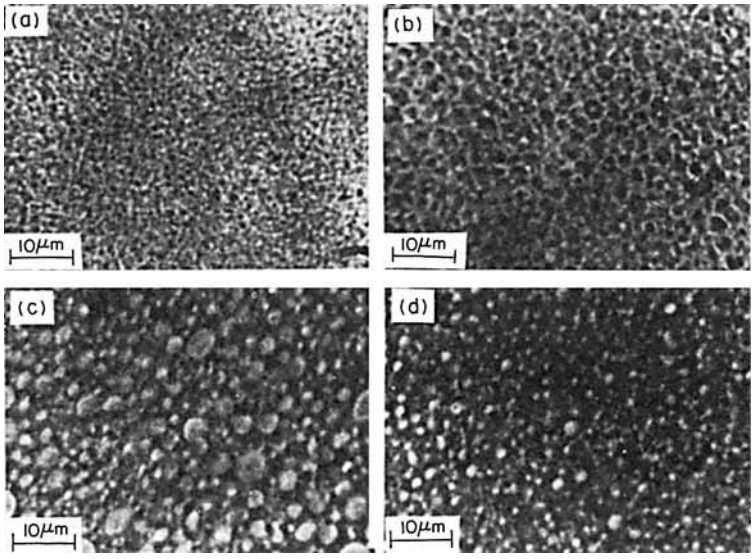

Fig. 5. Optical photomicrographs of nylon/CXA blend samples: (a) nylon/CXA = 20/80; (b) nylon/CXA = 40/60; (c) nylon/CXA = 60/40; (d) nylon/CXA = 80/20.

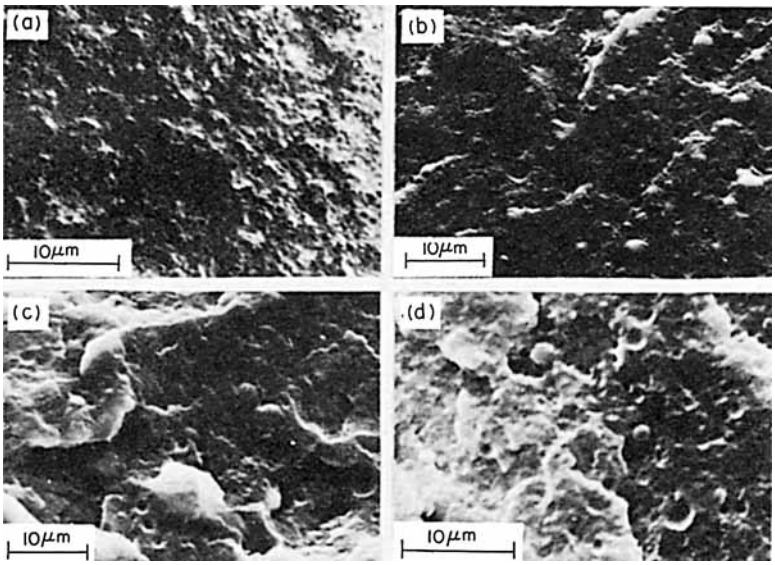

Fig. 6. Scanning electron micrographs obtained from cryogenically fractured samples of the blends; (a) nylon/CXA = 20/80; (b) nylon/CXA = 40/60; (c) nylon/CXA = 60/40; (d) nylon/CXA = 80/20.

the continuous phase (i.e., the CXA-rich blend), eq. (2) predicts a trend completely opposite to the experimental data. This implies that the discrete nylon phase is *not* bound loosely on the CXA matrix, and some adhesive force exists between the nylon and CXA phases.

Note that, in Figure 2, eq. (1) does not predict the experimental data well for the CXA-rich blends. However, eq. (3) can be made to fit the experimental data well by adjusting the value of ϕ_{max}. The ϕ_{max} values and the domain size of the discrete phase used, for calculating the modulus with the aid of eq. (3), are given in Table II. Note that a small ϕ_{max} value means a large volume at the interphase, which is immobilized by the discrete phase in the blend. The *reciprocal* of ϕ_{max} can be considered as an interaction parameter,[21,22] which is *proportional* to $[(R + \Delta R)/R]^3$, in which R is the radius of the inclusions and ΔR is the depth of the interphase, which is immobilized by the inclusions. For a given value of ΔR, the smaller the size of the inclusion, the smaller the ϕ_{max} value. This is the reason why the value of ϕ_{max} for the nylon-CXA = 40/60 blend in Table II is different from that for the nylon/CXA = 20/80 blend, although the extent of interaction (ΔR)

TABLE II
The Domain Size and the Maximum Packing Volume of the CXA-rich Blends

Blend composition (by wt)	Average domain size (μm)	Maximum packing volume fraction ϕ_{max}
Nylon/CXA = 40/60	5.0	0.40
Nylon/CXA = 20/80	1.5	0.25

between the two resins may be the same in these two blends. We presume here that the interphase is created from a grafted copolymer formed by nylon 6 and CXA3095, due to the high shear stress exerted on the materials during blending.

It is worth pointing out that some investigators[9,16] predicted rather successfully the moduli of particulate-filled composites, by using the van der Poel model[8] with $\phi_{max} = 0.6$ for hard inclusions and $\phi_{max} = 0.8$ for soft inclusions. When the van der Poel model was applied to our physical system under investigation, we observed a rather small (practically insignificant) improvement over the Kerner model. We believe that this is attributable to the small values of ϕ_{max} used, 0.25 for the nylon/CXA = 20/80 blend and 0.40 for the nylon/CXA = 40/60 blend, respectively (see Table II).

Compared to the well-developed theories for predicting the modulus of polymer blends, relatively little is available for predicting theoretically the tensile strength of polymer blends. According to Kunori and Geil[23] and Nielsen,[19] the tensile failure of a blend is attributable to the failure of the adhesion between the discrete phase and the continuous phase matrix, through crazing or a dewetting effect. The crazing or void depends on the area occupied by the discrete phase in the blend.

If there is little or no adhesive force existing between the constituent components in a blend, the tensile strength of the blend depends primarily on the continuous phase, and the tensile strength will go through a minimum, such as those observed in polystyrene/polypropylene and polystyrene/polyethylene blends.[24]

When there is no adhesive force between the constituents of a polymer blend, the tensile strength of the polymer blend may be represented by[23]

$$\sigma_b = \sigma_m(1 - A_d) \tag{7}$$

in which σ_b and σ_m are the tensile strength of the blend and the matrix, respectively, and A_d is the fraction of the area occupied by the discrete phase in the cross section of the specimen. On the other hand, when a strong adhesive force exists between the constituent components, the discrete phase will contribute to the tensile strength of the blend and eq. (7) may be modified as

$$\sigma_b = \sigma_m(1 - A_d) + \sigma_d A_d \tag{8}$$

in which σ_d denotes the tensile strength of the discrete phase.

According to Kunori and Geil,[23] when the tensile fracture loci propagate mainly through the interface, then A_d in eq. (8) varies with the two-thirds power of the volume fraction (type I fracture). However, when the fracture loci pass through the matrix for a considerable distance without intersecting a phase boundary, A_d varies with the first power of the volume fraction (type II fracture).

The micrographs describing the morphological state of the end surface of the tensile fractured specimen of the nylon/CXA = 80/20 and nylon/CXA = 60/40 blends are given in Figure 7. The measurement of the fraction of the area (A_d) occupied by the discrete phase (i.e., CXA particles) in this

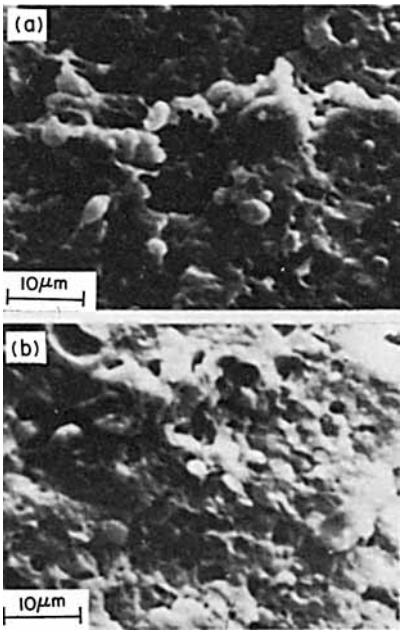

Fig. 7. Scanning electron micrographs of end surfaces of tensile fractured specimens: (a) nylon/CXA = 80/20; (b) nylon/CXA = 60/40.

figure is approximately proportional to the two-thirds power of the volume fraction (ϕ_d). This then indicates that type I fracture seems to prevail here and, therefore, the tensile strength of the blend under consideration may be described by

$$\sigma_b = \sigma_m(1 - \phi_d^{2/3}) + \sigma_d\phi_d^{2/3} \tag{9}$$

For the CXA-rich blends (i.e., CXA/nylon = 80/20 and 60/40), in which CXA3095 forms the continuous phase, the end surfaces of the tensile fractured specimen were so irregular, that pronounced fibrillar peaks were formed and, thus, gold coating was very difficult, not permitting us to look at the fractured surface with SEM. However, since the tensile strength of CXA3095 is quite low, we can speculate that the fracture will propagate through the CXA3095 matrix (continuous phase) and intersect with the domain boundary on its path, instead of perferentially propagating through the weak interface as in the case with the nylon-rich blends. Type II fracture may be applicable here, with the tensile strength represented by

$$\sigma_b = \sigma_m(1 - \phi_d) + \sigma_d\phi_d \tag{10}$$

Note that, in Figure 3, we used the tensile strength at the yield point of nylon 6 for calculating the tensile strength of the nylon/CXA = 80/20 and nylon/CXA = 60/40 blends, whereas the tensile strength at the break point of nylon 6 was used for calculating the tensile strengths of the nylon/CXA = 20/80 and 40/60 blends.

Impact Strength

The notched Izod impact strength of blend samples are plotted against blend composition in Figure 8. When 20 wt % of CXA 3095 was added to nylon 6, the impact strength was increased by approximately three times. However when 40 wt % of CXA3095 was added to the nylon 6, the impact strength was increased only by a factor of 2. It definitely shows impact modified behavior when the rubberlike CXA3095 was added to the rigid nylon 6.

It is seen that, for the nylon/CXA = 40/60 blend, the impact strength was increased sharply. We have experienced that for the nylon/CXA = 20/80 blend, the specimen not breaking at all. However, these two blends, in which the CXA3095 forms the continuous phase, are not discussed here because they are not considered to be impact-modified blends.

Stress whitening was observed with the specimens of the nylon/CXA = 80/20 and 60/40 blends over an area approximately 1 mm behind the notch. No stress whitening was observed in the fractured specimen of pure nylon 6. The stress whitening observed in the blend specimens is believed to arise from the formation of fibrils and domain deformation, debonding, and breaking as may be seen in Figure 9. In this figure, the fracture photomicrograph of the nylon 6 specimen is also shown for comparison purposes. It was observed further that, after the initial crack began, the crack propagated rapidly, but, in the area far behind the notch, the rubber particles failed to stop the crack and thus the fractured surfaces show a structure, as given in Figure 10. In other words, the impact fracture surface of blend specimens looks the same as that of pure nylon specimen, because the crack propagates through the nylon matrix. Thus it may be considered as brittle fracture.

Note in Figures 9(b) and 9(c) that part of the nylon 6 adheres to the

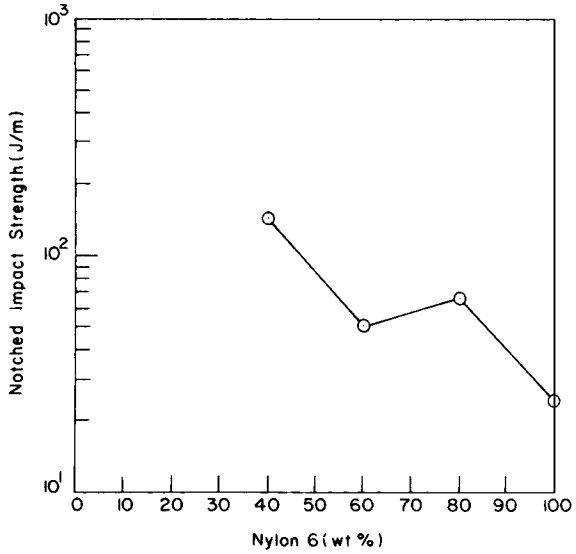

Fig. 8. Izod impact strength versus blend composition for the nylon/CXA blends.

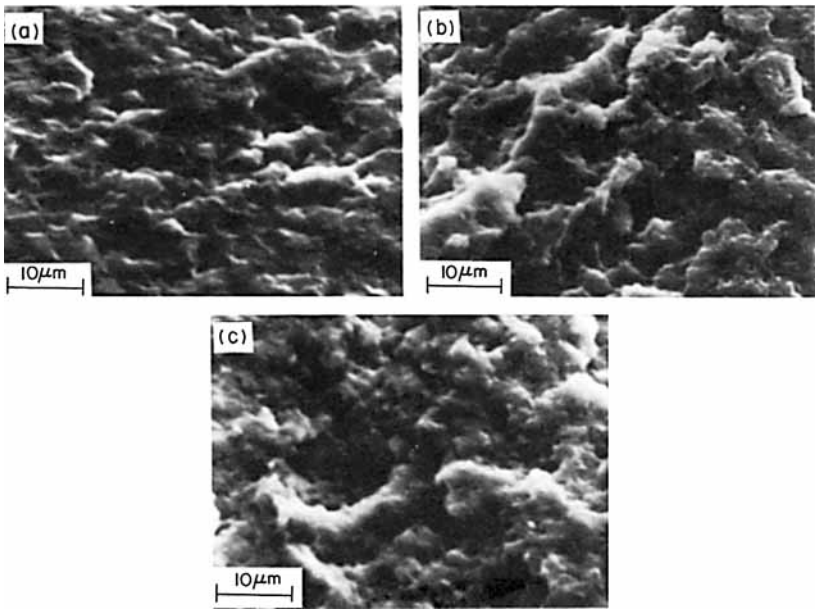

Fig. 9. Scanning electron micrographs of Izod impact fractured surface area *immediately behind* the notch: (a) nylon; (b) nylon-CXA = 80/20; (c) nylon/CXA = 60/40.

CXA3095 particles, indicating the existence of adhesion between the components. According to Wu[25] and Hobbs et al.,[26] the Izod impact strength of rubber-toughened nylon can be increased to 1100 J/m if the particle size is reduced to 0.3 μm. Wu[25] showed a ductile–brittle fracture transition zone

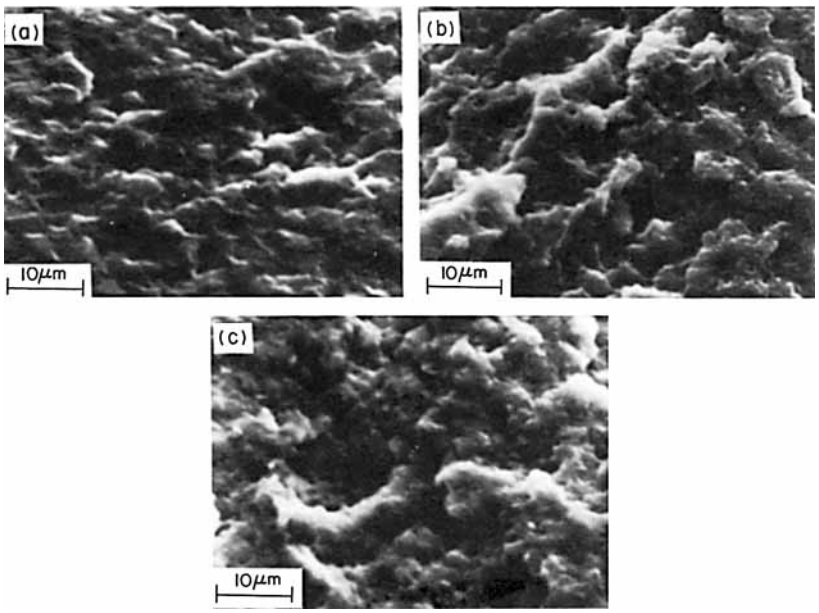

Fig. 10. Scanning electron micrographs of Izod impact fractured surfaces. Micrographs taken in the area *far behind* the notch: (a) nylon; (b) nylon/CXA = 80/20; (c) nylon/CXA = 60/40.

at a particle size of about 0.5 μm. When the ductile fracture prevails, all the fracture surface will be whitened.[26] Under such circumstances, the fractured structure, similar to that shown in Figures 10(b) and 10(c), would not exist. The fact that the impact strength depends on the particle size of the rubber phase helps us to explain why the nylon/CXA = 80/20 blend has greater impact strength than the nylon/CXA = 60/40 blend. Note that the nylon/CXA = 80/20 blend has smaller particles than the nylon/CXA = 60/40 blend (see Fig. 5).

References

1. E. H. Merz, G. C. Claver, and M. Baer, *J. Polym. Sci.*, **22**, 325 (1956).
2. W. Rovatti and E. G. Bobalek, *J. Appl. Polym. Sci.*, **7**, 2269 (1963).
3. R. Giuffria, *J. Appl. Polym. Sci.*, **7**, 1731 (1963).
4. K. Fujino, I. Owaga, and H. Kawai, *J. Appl. Polym. Sci.*, **8**, 2147 (1964).
5. M. Takayanagi, S. Eumura, and S. Minami, *J. Polym. Sci. Part C*, **5**, 113 (1964).
6. Z. Hashin and S. Shtrikman, *J. Mech. Phys. Solids*, **11**, 127 (1963).
7. E. H. Kerner, *Proc. Phys. Soc.*, **69B**, 808 (1956).
8. C. van der Poel, *Rheol. Acta*, **1**, 198 (1958).
9. J. C. Smith, *J. Res. Natl. Bur. Stand., Sect. A*, **78**, 355 (1974); **79**, 419 (1975).
10. Z. Hashin, *J. Appl. Mech.*, **29**, 143 (1962); **32**, 630 (1965).
11. T. Okamoto and M. Takayanagi, *J. Polym. Sci., Part C*, **23**, 597 (1968).
12. G. Kraus, K. W. Rollman, and J. T. Gruver, *Macromolecules*, **3**, 92 (1970).
13. K. Marcinin, A. Romanov, and V. Pollak, *J. Appl. Polym. Sci.*, **16**, 2239 (1972).
14. J. L. Work, *Polym. Eng. Sci.*, **13**, 46 (1973).
15. R. A. Dickie, *J. Appl. Polym. Sci.*, **17**, 45, 65, 79 (1973).
16. R. A. Dickie, *J. Polym. Sci., Polym. Phys. Ed.*, **14**, 2073 (1976).
17. C. D. Han, Y. J. Kim, and H. B. Chin, *Polym. Eng. Rev.* **4**, 177 (1984).
18. R. A. Dickie, in *Polymer Blends*, D. R. Paul and S. Newman, Eds., Academic, New York, 1978, Chap. 8.
19. L. E. Nielsen, *Mechanical Properties of Polymer and Composites*, Dekker, New York, 1974, Chap. 7.
20. B. Paul, *Trans. Metallurg. Soc. AIME*, **218**, 36 (1960).
21. K. D. Ziegel and A. Romanov, *J. Appl. Polym. Sci.*, **17**, 1119 (1973).
22. K. D. Ziegel and A. Romanov, *J. Appl. Polym. Sci.*, **17**, 1133 1973).
23. T. Kunori and P. H. Geil, *J. Macro Mol. Sci., Phys.*, **B18**(1), 135 (1980).
24. C. D. Han, C. A. Villamizar, and Y. W. Kim, *J. Appl. Polym. Sci.*, **19**, 2831 (1975).
25. S. Wu, *J. Polym. Sci., Polym. Phys. Ed.*, **21**, 699 (1983).
26. S. Y. Hobbs, R. C. Bopps, and V. H. Watkins, *Polym. Eng. Sci.*, **23**(7), 380 (1983).

Received November 21, 1983
Accepted May 17, 1984